Method for Ensuring Accurate AC Waveforms with Programmable Josephson Voltage Standards

Charles J. Burroughs, Jr., Alain Rüfenacht, Samuel P. Benz, *Member, IEEE* and Paul D. Dresselhaus

***Abstract*—The amplitudes of stepwise-approximated sine waves generated by programmable Josephson voltage standards (PJVS) are not intrinsically accurate because the transitions between the quantized voltages depend on numerous conditions. We have developed a method that ensures that the total rms output voltages of arbitrary ac waveforms synthesized by the PJVS are accurately referenced to the quantized Josephson voltages. This is accomplished by digitizing the output waveform, utilizing the quantized voltages to correct digitizer gain, noise, and nonlinearity, and then utilizing measurements of the bandwidth, rise time, and harmonic content to precisely tune the PJVS bias parameters. Our goal is to develop an AC standard source that can directly synthesize voltages with the accuracy expected of a quantum-based standard without the use of a thermal voltage converter.**

***Index Terms*—Josephson arrays, Josephson device measurement applications, Josephson devices, Josephson voltage standard, measurement standards.**

I. Introduction

Since the introduction of series arrays of intrinsically shunted Josephson junctions in the mid-1990s [1]–[3], PJVS systems have utilized selectable sets of junction arrays to generate stepwise-approximated waveforms with the intent of bringing quantum-based accuracy to the field of ac voltage metrology. Significant progress has been made for a number of ac metrology applications, most usefully with sampled comparisons [4]–[10] and for (50–60 Hz) power metrology [11], [12]. Unfortunately, the inherent error in the output voltage caused by the transitions between the quantized voltages [13], [14] has remained a fundamental and unsolved weakness. Consequently, thermal voltage converters (TVCs) remain the primary standards for ac voltage worldwide. Various measurement schemes have been investigated that utilize combinations of TVCs and stepwise PJVS synthesized waveforms working together [15], [16]. However, the previous techniques that have exploited PJVS waveforms have not provided the required accuracy at frequencies above 100 Hz without utilizing a TVC.

PJVS-synthesized waveforms are fundamentally different from the harmonically pure tones produced by the ac Josephson voltage standard that is based on high-speed pulse-driven arrays [17] that typically produce signals in the frequency range from dc to 100 kHz and have output voltages up to a few hundred millivolts. The main advantage of PJVS systems is their significantly larger output amplitude up to 10 V [18]. The PJVS output waveforms are constructed with quantized voltages from multiple Josephson-junction series arrays driven by a continuous microwave signal. This approach offers the promise of an accurate ac and dc voltage source for frequencies below a few kilohertz, but unfortunately, the PJVS stepwise-synthesis method has a critical limitation in that the output voltage is not precisely known during the transitions between the quantized voltages. More importantly, the generated rms voltage depends on the exact timing of the bias-current transitions, as have been previously described [13]–[16]. The transition timing is affected by (a) the precise shape of the voltage-current (VI) characteristic of each Josephson sub-array, (b) the values chosen for bias-current setpoints, and (c) any variations in the delivered bias currents from those target values, such as bias settling behavior and interactions during transitions between bias signals and/or drive channels. Furthermore, any changing environmental or bias condition, such as a change in the microwave power, chip temperature, or dewar pressure, that changes either the VI characteristics or the bias-current setpoints changes the transition timing (and to a lesser degree the transition shape) and significantly alters the rms voltage of the stepwise-approximated ac waveform.

II. Transition-Related Errors in PJVS Waveforms

The dependence on transition-timing causes the PJVS rms output voltage to depend simultaneously on numerous bias and environmental conditions. For rms measurements, the PJVS should therefore be considered an adjustable voltage source (not an intrinsically accurate ac standard), because it generates a relatively stable, nearly accurate waveform, but its stability and accuracy depend on the many conditions described above. Thus, PJVS systems do not qualify as intrinsic ac voltage standards because they cannot produce rms amplitudes that are calculable only from the Josephson quantization.

The details of how changes in PJVS bias parameters cause a shift in the timing of the transitions have been previously discussed in detail [13], [14]. Fig. 1 illustrates how transition timing affects the total rms voltage for an example waveform with only four steps. The fully settled quantized voltages of the PJVS are labeled S1 through S4, and the transitions between

Manuscript received July 2, 2012; revised January 5, 2013; accepted January 8, 2013. Date of publication April 9, 2013; date of current version May 8, 2013. The Associate Editor coordinating the review process was R. Landim.

The authors are with the National Institute of Standards and Technology, Boulder, CO 80305, USA.

Color versions of one or more of the figures in this letter are available online at http://ieeexplore.ieee.org.

Digital Object Identifier 10.1109/TIM.2013.2250192

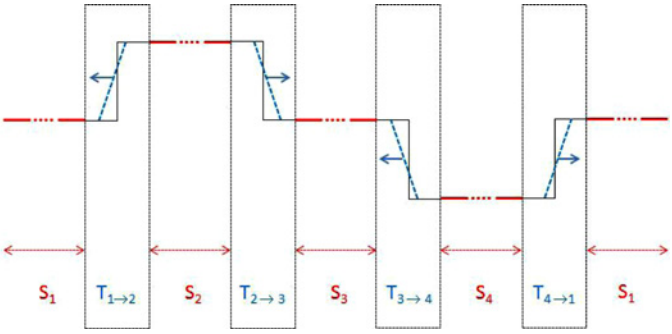

Fig. 1. Transition timing changing the total rms voltage of a PJVS waveform.

those voltages are designated $T_{(n\rightarrow n+1)}$. An increase in the bias-current setpoint, which is the current simultaneously biasing all the PJVS sub-arrays, for example, causes transitions $T_{(1\rightarrow 2)}$ and $T_{(3\rightarrow 4)}$ to both occur slightly earlier in time (shifting left in Fig. 1), while transitions $T_{(2\rightarrow 3)}$ and $T_{(4\rightarrow 1)}$ both occur slightly later in time (shifting right in Fig. 1). Although the transition timing may shift by only a fraction of a nanosecond, the resulting change in total rms voltage is significant when the PJVS waveform frequency is in the audio range (causing errors up to $\pm 20\,\mu$V/V at 1 kHz for our system).

The error introduced by the transitions arises because the contribution to the total rms voltage of the sloped waveform transitions (dashed blue lines) shown in the rectangles of Fig. 1 differs from the contribution to the total rms voltage of the instantaneous waveform transitions (solid black vertical lines) shown in the rectangles. This error in the PJVS ac output voltage is adjustable as a function of various bias parameters, and it scales directly with the frequency of the PJVS waveform. For example, the plot of the rms voltage versus dither current (an offset applied to the bias-current setpoint of all sub-arrays simultaneously) at 1 kHz will have a specific slope (related to the rise time of the bias electronics), and at 2 kHz (and 3 kHz) the measured slope will be exactly two times (and three times) higher. There are combinations of bias parameters where these curves of different slopes intersect each other, and there is often a significant range of PJVS waveform frequencies where the curves intersect near a common point, as many PJVS researchers have observed [13]–[16]. We designate such a combination of bias settings as the special operating point (SpOpPt); it is special because the synthesized PJVS waveform (blue) in Fig. 1 has been adjusted so that its total rms voltage is identical to that of the ideal waveform (black) in Fig. 1. At the SpOpPt, the total rms voltage at any PJVS output frequency is exactly the same as an ideal PJVS stepwise waveform with zero-nanosecond transitions between steps (with the same voltages).

To find the SpOpPt, we must find a setting of bias parameters where the frequency dependence of the PJVS output goes to zero. This sounds simple enough, but identifying the true SpOpPt requires careful and extensive measurements to ensure self-consistency, because even the best instruments available for measuring the PJVS rms voltage have finite bandwidths as well as amplitude- and frequency-dependent non-idealities. This means that the bias settings that produce the best agreement between multiple PJVS waveform frequencies are actually the settings where the frequency dependence of the measuring instrument most closely opposes the frequency-dependent error of the PJVS total rms voltage. So, to find the true SpOpPt, we must know with certainty the frequency response of the measuring instrument, and carefully correct for that error. In this letter, which was presented at the CPEM 2012 conference with a brief summary in the proceedings [19], we explain in detail a method for adjusting the output voltage of the PJVS and accurately determining its rms value. Our method determines the SpOpPt through measurements of PJVS waveforms of different frequencies by analyzing and correcting for time-, amplitude-, and frequency-dependent variations of the PJVS system and sampling analog-to-digital converter (ADC). A simplified overview of the measurement setup is shown in Fig. 2.

III. Error Correction Method

In pursuit of an accurate determination of the PJVS synthesized rms voltage without the use of a TVC, we optimize the following procedure: (a) digitize the stepwise PJVS output waveform with a sigma-delta ADC, (b) calibrate and remove any time-dependent drift in the sections of the fully settled steps, based on their known quantized voltages, to correct the gain and dc offset of the digitizer, (c) average hundreds of waveform cycles to reduce measurement noise and correct small nonlinearities of the digitizer, and (d) account for effects due to the transfer function of the digitizer and measurement leads. All this data processing yields a value for the rms voltage of the PJVS waveform (V_{rms}), but the analysis also requires careful evaluation of systematic errors in the complex measurement process.

A. Time-Domain Calculations

The digitizer utilizes its ± 5 V range to measure the full amplitude of the PJVS waveform. It measures a continuous stream of many cycles of the PJVS waveform three separate times, each with a different sample rate setting (f_s = 1 MHz, 2 MHz, and 4 MHz). We presently utilize an NI-5922[1] digitizer that operates at an oversampling rate of 120 MHz, and processes the data into the average value of the input voltage during each sample interval (1 μs, 500 ns, and 250 ns, respectively). We synchronize the PJVS waveform to the sample intervals such that the transitions in the PJVS stepwise waveform occur near the edge of the sample intervals, thus the value in the sample interval most closely represents rms value. (For the PJVS waveforms we discuss in this letter, the sampled voltages are effectively equivalent to the rms voltage, where the difference is more than an order of magnitude smaller than the other dominant sources of uncertainty.) The digital filter

[1]Certain commercial equipment, instruments, or materials are identified in this report to facilitate understanding. Such identification does not imply recommendation or endorsement by NIST, nor does it imply that the materials or equipment that are identified are necessarily the best available for the purpose.

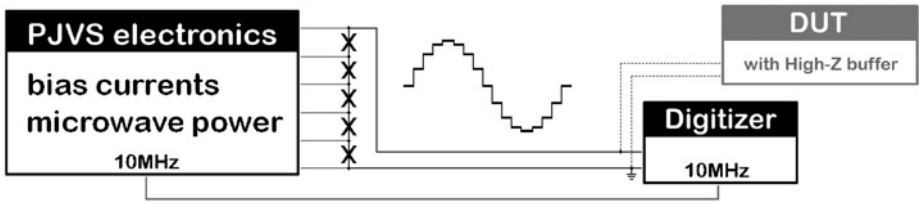

Fig. 2. Block diagram of the PJVS measurement system utilizing a 3.9 V Josephson array measured by a digitizer. The location of a device under test (DUT) with high impedance buffer amplifier, if required, is also shown for illustrative purposes although for the experiments in this letter the DUT was not connected. To ensure that the digitizer and the DUT receive the same input voltage waveform, the connection between them would need to be as short as possible, using a coaxial tee for example.

selected is the 48-tap standard, the filter option with flattest pass-band for our particular digitizer. The first PJVS cycle in each data stream is discarded to reject startup variations in the digitizer measurement. Since the digitizer and the PJVS waveform are locked to a common 10 MHz clock, we can reduce the multiple PJVS cycles in each data stream into a single combined PJVS cycle by averaging corresponding samples in each of the n cycles. This time-domain technique averages the noise, digitizer gain drift, and digitizer dc-offset drift in a single step, and proved superior to several other methods that were attempted to measure and correct for these non-idealities.

The following procedure describes how these non-idealities are removed from the measured data. For each combined PJVS cycle, we compare the measured voltages at each step of the stepwise-approximated waveform with the known values of the quantized voltages to calculate the gain and dc-offset corrections to be applied to the center samples of each waveform step. Applying an individual correction to each waveform step has the added benefit of removing nonlinearities of the digitizer [20]. The values of the remaining samples of the combined PJVS cycle that reside between the fully settled PJVS voltages (including those samples containing the transitions) are adjusted by interpolating between the gain correction factors of their adjacent steps. After the gain corrections are applied to each sample of the combined PJVS cycle, the data processing in the time domain is complete, and the rms voltage is calculated. In successive measurements, using this method we typically observe scatter less than 100 nV over the timespan of an hour, which is small enough to support the frequency-domain analysis that follows.

The time-domain-corrected PJVS waveform cycle is an intermediate step in the SpOpPt procedure that occurs before the frequency-domain analysis and corrections are performed; some example time-domain-corrected results are presented in Fig. 3 to illustrate some key features. Fig. 3(a) shows the PJVS rms voltage, determined from the time-domain-corrected PJVS cycle analyses described above, measured by the digitizer at f_s = 4 MHz at several PJVS output frequencies as a function of dither current. These curves intersect in a relatively tight region near a setpoint value of 0.45 mA. However, drawing conclusions about the rms voltage value from how closely the various PJVS frequency points land on top of each other is premature, because some of the harmonic content in the PJVS waveform is outside the digitizer bandwidth and thus not included in the measured V_{rms}. Similarly, there is a tight

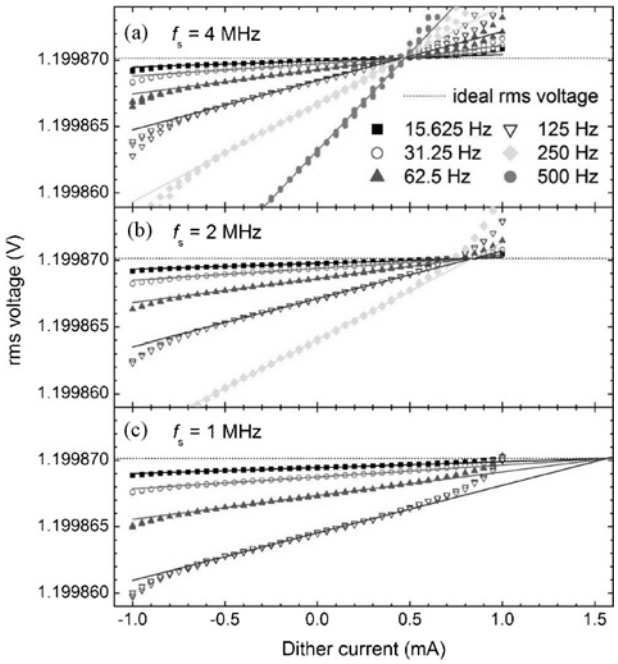

Fig. 3. Measured PJVS total rms voltage as a function of dither current (applied to all sub-arrays simultaneously) for stepwise sine wave with 64 steps and rms amplitude of 1.2 V. The time domain data processing of these data is complete, but the frequency-domain corrections for the transfer function of the digitizer have not been applied.

intersection of the different curves in "Fig. 3(b)" at 0.75 mA (f_s = 2 MHz) and in Fig. 3(c) at 1.0 mA (f_s = 1 MHz). The fact that these intersection points occur at different values of dither current for the different sampling frequencies clearly indicates that another systematic correction is required to correctly determine the total V_{rms} of the PJVS source and demonstrates a self-consistent measurement procedure. In the following section III-C, we show that accounting for the harmonic content can resolve this discrepancy.

In Fig. 3(c), the data values intersect at a dither current of +1 mA, which actually biases the PJVS just outside the flat region of PJVS steps where the voltage is quantized. The error in total V_{rms} caused by the transitions scales directly with PJVS waveform frequency, because the fraction of time the waveform is making step transitions is increasing with frequency. At very low PJVS waveform frequencies (a few Hz for example), the intersection points always converge to the ideal value, i.e., the value given by instantaneous transitions of 0 ns (unattainable by a real PJVS system). The tight intersec-

tions in Fig. 3 occur at a setpoint where the PJVS-frequency-dependent error in measured V_{rms} due to the missing harmonic content is compensated by a PJVS-frequency-dependent error due to the PJVS transition time placement. Since the amount of missing harmonic content increases for lower sampling rates of the digitizer, the intersection point appears at higher dither currents as the sampling frequency decreases. In the following section, we show that to find the true SpOpPt for total rms voltage of the PJVS source, we must properly account for the measured harmonic content and determine a dither current value that is identical for all three digitizer sample rates.

B. Frequency-Domain Calculations

A stepwise-approximated waveform synthesized by a PJVS source deviates from its ideal waveform in many ways, including the rise time transitions produced by the PJVS bias system and the shifts in time placement of those transitions as a function of various bias parameters. When a PJVS waveform is measured by another instrument, the amplitude and frequency response of the instrument (and the measurement leads) must also be considered. The measured V_{rms} is dependent on the measurement bandwidth and transfer function of the digitizer because it modifies the measured harmonic content by modifying the amplitudes of the in-band harmonics and removing the out-of-band harmonic content entirely. With our knowledge of the digitizer response as a function of frequency (in the pass-band and in the vicinity of the cutoff frequency) and the PJVS rise time and calculated harmonic spectrum, we can apply corrections to the measured V_{rms} values that restore the contributions of the harmonics that are modified by the digitizer.

Fig. 4 shows the transfer function of the digitizer when utilizing its 48-tap standard digital filter, which is the flattest pass-band presently available for our particular digitizer. We measured this transfer-function behavior directly for different sampling frequencies by sweeping the frequency of a sine wave tone through the pass-band and past the Nyquist frequency. The sine wave was generated by a calibrator, so we expect the uncertainty of the transfer function to easily be within $\pm 100\,\mu$V/V. Our software implementation of this transfer function is consistent with both the experimental data and the published characteristic from the digitizer manufacturer. The cutoff frequency is clearly visible at the Nyquist frequency $f/f_s = 0.5$, as expected. Notice that the digital filter has small amplitude variations in the nominally flat pass-band (dc to 400 kHz) region that must be included in the analysis [see the zoomed view in Fig. 4(a)]. The calculated harmonic content of a PJVS stepwise-approximated waveform (20 ns rise time) is superimposed on the filter transfer function in Fig. 4 to illustrate the impact the digitizer transfer function has on the measured waveform. Fig. 4 also aids in considering the effect of the uncertainty of the measured transfer function. For example, the first digitization harmonic in Fig. 4 is 0.02 V, and if our transfer function model differed from the actual digitizer performance by $+100\,\mu$V/V at that frequency, the peak would measure 0.020 002 V, which would increase the total rms voltage by $0.03\,\mu$V/V. Even if all digitization harmonics within the digitizer bandwidth measured $100\,\mu$V/V higher than their actual amplitude, the increase in total rms voltage would be

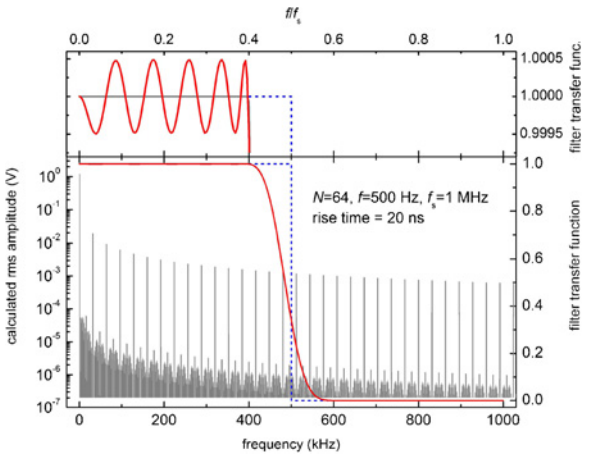

Fig. 4. Measured transfer function for our digitizer utilizing its 48-tap standard digital filter. This same frequency response relative to normalized frequency f/f_s was observed for all three sampling frequencies used in our measurements, f_s = (1, 2, and 4) MHz. Also shown is the calculated spectrum for a PJVS stepwise-approximated sine wave with 64 steps at a 500 Hz fundamental frequency.

less than $0.1\,\mu$V/V so this potential source of error is presently below our dominant sources of uncertainty, but we must be mindful to use a large enough number of samples to keep the error negligible. Another aspect of the transfer function that we must verify is aliasing, where the digitization harmonics just above the cutoff frequency are folded back into the pass band. Fortunately, when we choose the number of steps in the PJVS stepwise waveform, we know exactly the frequency of all the digitization harmonics, and we can easily arrange for the aliased harmonics to land at different frequencies than the in-band harmonics. This allows us to directly observe the aliased tones and verify that they are sufficiently attenuated to be negligible.

The results of the fast fourier transform (FFT) calculations depend on the rise time between PJVS quantized steps. Measurements of the rise time of our PJVS output voltages give a value of 20 ns $\pm$5 ns. To correct the total rms voltage for the missing harmonic content and determine the setting of the bias parameters that corresponds to the true SpOpPt, we calculate the Fourier spectrum of the ideal stepwise waveform assuming a 20 ns rise time. We also calculate the corrected rms voltages for the two rise times at the 20 $\pm$5 ns upper and lower limits, which results in a Type B component for our overall uncertainty budget. Another critical aspect of our error correction method to consider is how the PJVS frequency spectrum is affected when we adjust the PJVS rms voltage by changing one or more bias parameters (typically rf power level and/or the bias current setpoints). We utilized several models to explore this issue and have found that, for our 20 ns rise time, the 1 ns to 2 ns shifts in transition timing (produced by varying the bias parameters) change the total PJVS output V_{rms} by similarly affecting both the fundamental amplitude and all the harmonics, such that their ratios are virtually identical. Changing the rise time by $\pm$5 ns, however, alters the spectrum sufficiently that we must account for the uncertainty in the rise time in our uncertainty analysis.

TABLE I

TYPICAL TYPE B UNCERTAINTIES ASSIGNED TO THE SPOPPT SETPOINT

PJVS waveform steps (n)	Uncertainty in SpOpPt setpoint due to rise time range of PJVS transitions (Type B)	Uncertainty in SpOpPt setpoint due to discrepancy at various samples reates (Type B)	Uncertainty in SpOpPt setpoint due these two factors combined (Type B)	Resulting Uncertainty in PJVS total rms voltage due to the two factors (Type B)
32	± 0.025 mA	± 0.01 mA	± 0.035 mA	± 0.84 μV/V per kHz
40	± 0.020 mA	± 0.01 mA	± 0.030 mA	± 0.72 μV/V per kHz
64	± 0.010 mA	± 0.01 mA	± 0.020 mA	± 0.48 μV/V per kHz
128	± 0.005 mA	± 0.01 mA	± 0.015 mA	± 0.36 μV/V per kHz

(Columns 2 and 3 are max/min values obtained via the analysis of measured data. Consequently, columns 4 and 5 are also max/min.)

TABLE II

UNCERTAINTY BUDGET FOR THE TOTAL V_{rms} OF A PJVS SOURCE WHEN GENERATING STEPWISE SINE WAVES AT THE SPOPPT, UTILIZING THE FULL ERROR CORRECTION METHOD. THESE DATA CORRESPOND TO THE EXAMPLE OF FIGS. 3 AND 5 FOR A STEPWISE SINE WAVE WITH 64 STEPS AND RMS AMPLITUDE OF 1.2 V

PJVS fundamental frequency (f)	Type A Uncertainty (measured scatter in repeated measurements of Vrms at fixed SpOpPt)	Type B Uncertainty (calculated from *Table I* above)	**Resulting Total Uncertainty of PJVS Vrms output**
250 Hz	± 0.07 μV/V	± 0.12 μV/V	± **0.2** μ**V/V**
500 Hz	± 0.15 μV/V	± 0.24 μV/V	± **0.4** μ**V/V**
1 kHz	± 0.3 μV/V	± 0.48 μV/V	± **0.8** μ**V/V**
2 kHz (predicted)	± 0.6 μV/V	± 0.96 μV/V	± **1.6** μ**V/V**
5 kHz (predicted)	± 1.5 μV/V	± 2.4 μV/V	± **3.9** μ**V/V**

(Columns 2 and 3 are max/min values obtained via the analysis of measured data. Consequently, column 4 is also max/min.)

TABLE III

CALCULATED HARMONIC CONTENT FOR A PJVS STEPWISE-APPROXIMATED 1 KHZ SINE WAVES WITH VARIOUS NUMBERS OF SAMPLES (20 NS RISE TIME)

PJVS waveform steps *(n)*	Amount of total rms voltage in *all* harmonics	Amount of total rms voltage in harmonics above 500 kHz	Amount of total rms voltage harmonics above 1 MHz	Amount of total rms voltage in harmonics above 2 MHz
64	**400** μ**V/V**	31.5 μV/V	14.8 μV/V	6.8 μV/V
128	**100** μ**V/V**	16.8 μV/V	7.6 μV/V	3.5 μV/V
250	**26** μ**V/V**	8.1 μV/V	3.8 μV/V	1.8 μV/V
500	**6.5** μ**V/V**	4.4 μV/V	2.0 μV/V	0.89 μV/V
1000	**1.6** μ**V/V**	1.6 μV/V	1.1 μV/V	0.46 μV/V

In Fig. 5, we show the frequency-domain corrected total V_{rms} values for the example data of Fig. 3. These results show a dramatic improvement in that the intersection of the traces for different PJVS frequencies occurs at nearly the same dither current operating point for all the three digitizer sampling rates. This 0.165 mA common operating point demonstrates that consistent total V_{rms} results are obtained for the different measurement bandwidths and sampling rates. However, the SpOpPt values are not quite identical for the different digitizer sampling rates, so the small discrepancies produce another Type B uncertainty term. Table I summarizes our estimates of Type B uncertainties for several stepwise waveforms for our PJVS system. To summarize the measurement sequence that resulted in this table, a specific PJVS waveform is produced at several different PJVS frequencies (in the example case of Figs. 3 and 5, stepwise sine waves with an rms amplitude of 1.2 V and 64 steps), and each waveform is measured by the digitizer at several sampling rates. A bias parameter, in this case dither current, is varied to locate the setting that produces the SpOpPt. The Type B uncertainties at this stage of the analysis have the same units (milliamperes) as the parameter that was varied. Finally, the Type B values are converted into a voltage uncertainty, as shown in the last column of Table I. This conversion is accomplished by multiplying the measured slopes of the data (12 μV/V per mA at 500 Hz, etc…) by the Type B quantity in column four. Notice in column two that the Type B uncertainty decreases with increasing number of steps in the PJVS waveform because the harmonic amplitudes decrease for these waveforms.

C. Uncertainty Calculations

For the PJVS to perform precision measurements with another instrument that is simultaneously connected [such as the device under test (DUT) in Fig. 1], we must adjust the bias parameters to attain the SpOpPt, and then we must provide a complete uncertainty budget for the PJVS output at each voltage, waveform, and frequency. At the higher frequencies (1 kHz to 10 kHz) where this direct-synthesis SpOpPt method is more challenging, the short-term (30 min) stability of the bias parameters must be considered. For example, as the microwave amplifier gradually warms up after being switched on, the microwave power will be slowly changing, which requires that we periodically select a slightly different setting of the bias parameters to reposition the SpOpPt. Such drift in the bias parameters is a source of uncertainty that must be taken into account. In addition, we

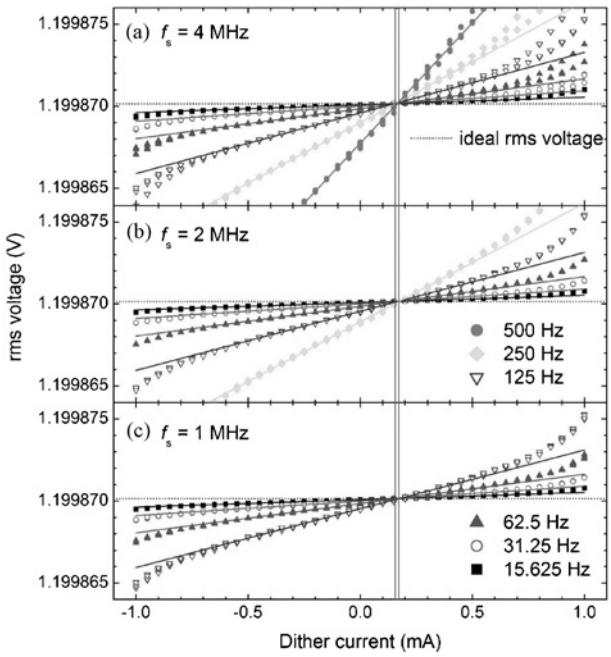

Fig. 5. Measured PJVS total rms voltage as a function of dither current (applied to all sub-arrays simultaneously) for stepwise sine wave with 64 steps and rms amplitude of 1.2 V. The full data processing algorithm has been applied (both time-domain and frequency-domain corrections).

must also consider the jitter associated with the bias parameter settings.

One method for characterizing the stability of the SpOpPt is to simply measure V_{rms} repeatedly (utilizing the entire error correction method) at a number of PJVS output frequencies, preferably at frequencies above 1 kHz, where the stability is the most critical. Some typical stability results are shown in Table II, where column two is the max/min scatter observed in the repeated measurements of total V_{rms} (with the full time-domain and frequency-domain analysis performed). Once the operating temperatures of the PJVS system components and measurement instruments come to thermal equilibrium, the typical stability of the bias parameters is revealed by the Type A scatter in Table II. In practice, we measure the Type A scatter for several minutes at various PJVS frequencies with both the digitizer and DUT connected, and determine whether the SpOpPt remained sufficiently constant, and collect the data for calculating the SpOpPt uncertainties.

IV. Future Direction

We believe that further optimization of the SpOpPt method will enable the reduction of the Type B uncertainties in column three of Table II by a factor of 2 or 3, primarily by operating with a larger number of PJVS steps and optimizing the data processing algorithm. By properly correcting the various non-idealities of the digitizer, and carefully accounting for harmonic content and bandwidth, we believe that the SpOpPt measurement method will be capable of producing rms voltages that are accurate to a few 0.1 μV/V at 1 kHz. This will allow us to finally reach our objective [1] of creating PJVS stepwise synthesized waveforms with calculable rms voltages without the use of either ac-dc transfer comparisons or a TVC reference. Another advantage of increasing the number of PJVS steps is that the harmonic content of the waveforms will be greatly reduced. Table III illustrates that the contribution to the total rms voltage from all the harmonic content in a stepwise-approximated 1 kHz sine wave with 1000 Josephson steps is only 1.6 μV/V.

V. Conclusion

We have demonstrated a method for tuning a PJVS so that it synthesizes ac waveforms with calculable and accurate rms voltages. The method utilizes the quantized voltages of stepwise-approximated waveforms produced by the PJVS to characterize the gain and offsets of a sampling ADC. We determine the total PJVS rms output voltage utilizing the measured waveform from the calibrated ADC, the measured ADC frequency response, and the PJVS measured rise time and calculated harmonic content. Further research is required to investigate other potential systematic error sources, and to develop a more comprehensive uncertainty budget. We are hopeful that this method will enable the PJVS to be a practical AC standard source suitable for voltage metrology with an accuracy of a few 0.1 μV/V at 1 kHz. Ultimately, we expect that the system computer could utilize this method to locate the SpOpPt automatically, and also perform the necessary measurements for calculations of the uncertainty.

Acknowledgments

The authors would like to thank Y. Chong, N. Hadacek, B. Baek, and M. Watanabe for helping develop the stacked-junction fabrication process for our PJVS chips, and B. Waltrip for collaborative discussions about various digital sampling technologies.

References

[1] C. A. Hamilton, C. J. Burroughs, and R. L. Kautz, "Josephson D/A converter with fundamental accuracy," *IEEE Trans. Instrum. Meas.*, vol. 44, no. 2, pp. 223–225, Apr. 1995.

[2] S. P. Benz, C. A. Hamilton, C. J. Burroughs, T. E. Harvey, and L. A. Christian, "Stable 1-volt programmable voltage standard," *Appl. Phys. Lett.*, vol. 71, pp. 1866–1868, Sep. 1997.

[3] H. Schulze, R. Behr, F. Müller, and J. Niemeyer, "Nb/Al/AlO/Al/AlO/Al/Nb Josephson junctions for programmable voltage standards," *Appl. Phys. Lett.*, vol. 73, pp. 996–998, Aug. 1998.

[4] R. Behr, L. Palafox, G. Ramm, H. Moser, and J. Melcher, "Direct comparison of Josephson waveforms using an ac quantum voltmeter," *IEEE Trans. Instrum. Meas.*, vol. 56, no. 2, pp. 235–238, Apr. 2007.

[5] A. Rüfenacht, C. J. Burroughs, and S. P. Benz, "Precision sampling measurements using ac programmable Josephson voltage standards," *Rev. Sci. Instrum.*, vol. 79, no. 4, pp. 044 704-1–044 704-9, Apr. 2008.

[6] A. Rüfenacht, C. J. Burroughs, S. P. Benz, P. D. Dresselhaus, B. C.Waltrip, and T. L. Nelson, "Precision differential sampling measurements of low-frequency synthesized sine waves with an ac programmable Josephson voltage standard," *IEEE Trans. Instrum. Meas.*, vol. 58, no. 4, pp. 809–815, Apr. 2009.

[7] M.-S. Kim, K.-T. Kim, W.-S. Kim, Y. Chong, and S.-W. Kwon, "Analog-to-digital conversion for low-frequency waveforms based on the Josephson voltage standard," *Meas. Sci. Technol.*, vol. 21, no. 11, pp. 115102-1–115102-6, 2010.

[8] J. M. Williams, D. Henderson, J. Pickering, R. Behr, F. Müller, and P. Scheibenreiter, "Quantum-referenced voltage waveform synthesiser," *IET Sci. Meas. Technol.*, vol. 5, no. 5, pp. 163–174, 2011.

[9] I. Budovsky, D. Georgakopoulos, T. Hagen, H. Sasaki, and H. Yamamori, "Precision ac-dc difference measurement system based on a programmable Josephson voltage standard," *IEEE Trans. Instrum. Meas.*, vol. 60, no. 7, pp. 2439–2444, Jul. 2011.
[10] A. Rüfenacht, F. Overney, A. Mortara, and B. Jeanneret, "Thermal transfer standard validation of the Josephson-voltage-standard-locked sine wave synthesizer," *IEEE Trans. Instrum. Meas.*, vol. 60, no. 7, pp. 2372–2377, Jul. 2011.
[11] L. Palafox, G. Ramm, R. Behr, W. G. Kürten Ihlenfeld, and H. Moser, "Primary ac power standard based upon programmable Josephson junction arrays," *IEEE Trans. Instrum. Meas.*, vol. 56, no. 2, pp. 534–537, Apr. 2007.
[12] C. J. Burroughs, S. P. Benz. P. D. Dresselhaus, B. C. Waltrip, T. L. Nelson, Y. Chong, J. M. Williams, D. Henderson, P. Pratel, L. Palafox, and R. Behr, "Development of a 60 Hz power standard using SNS programmable Josephson voltage standards," *IEEE Trans. Instrum. Meas.*, vol. 56, no. 2, pp. 289–294, Apr. 2007.
[13] C.J. Burroughs, A. Rüfenacht, S. P. Benz, P. D. Dresselhaus, B. C. Waltrip, and T. L. Nelson, "Error and transient analysis of stepwise-approximated sine waves generated by programmable Josephson voltage standards," *IEEE Trans. Instrum. Meas.*, vol. 57, no. 7, pp. 1322–1329, Jul. 2008.
[14] C. J. Burroughs, A. Rüfenacht, S. P. Benz, and P. D. Dresselhaus, "Systematic error analysis of stepwise-approximated ac waveforms generated by programmable Josephson voltage standards," *IEEE Trans. Instrum. Meas.*, vol. 58, no. 4, pp. 761–767, Apr. 2009.
[15] O. Séron, S. Djordjevic, I. Budovsky, T. Hagen, R. Behr, and L. Palafox, "Precision ac–dc transfer measurements with a Josephson waveform synthesizer and a buffer amplifier," *IEEE Trans. Instrum. Meas.*, vol. 61, no. 1, pp. 198–204, Jan. 2012.
[16] G. Eklund, T. Bergsten, V. Tarasso, and K. Rydler, "Determination of transition error corrections for low-frequency stepwise-approximated Josephson sine waves," *IEEE Trans. Instrum. Meas.*, vol. 60, no. 7, pp. 2399–2403, Jul. 2011.
[17] S. P. Benz, P. D. Dresselhaus, A. Rüfenacht, N. F. Bergren, J. R. Kinard, R. P. Landim, and T. L. Nelson, "Progress toward a 1 V pulse-driven ac Josephson voltage standard," *IEEE Trans. Instrum. Meas.*, vol. 58, no. 4, pp. 838–843, Apr. 2009.
[18] C. J. Burroughs, P. D. Dresselhaus, A. Rüfenacht, D. Olaya, M. M. Elsbury, Y. Tang, and S. P. Benz, "NIST 10 V programmable Josephson voltage standard system," *IEEE Trans. Instrum. Meas.*, vol. 60, no. 7, pp. 2482–2488, Jul. 2011.
[19] C. J. Burroughs, A. Rüfenacht, S. P. Benz, and P. D. Dresselhaus, "Method for ensuring accurate ac waveforms with programmable Josephson voltage standards," in *Proc. Conf. Precision Elec. Meas.*, Washington DC, USA, 2012, July 2–6.
[20] F. Overney, A. Rüfenacht, J. Braun, B. Jeanneret, and P. S. Wright, "Characterization of metrological grade analog-to-digital converters using a programmable Josephson voltage standard," *IEEE Trans. Instrum. Meas.*, vol. 60, no. 7, pp. 2172–2177, Jul. 2011.

Charles J. Burroughs, Jr. was born on June 18, 1966. He received the B.S. degree in electrical engineering from the University of Colorado, Boulder, CO, USA, in 1988.

He is currently with the National Institute of Standards and Technology (NIST), Boulder, where he was first a student and has been a permanent Staff Member since 1988. At NIST, he has worked in the area of superconductive electronics, including the design, fabrication, and testing of Josephson voltage standards, and digital-to-analog and analog-to-digital converters. He has authored 45 publications and holds three patents in the field of superconducting electronics.

Mr. Burroughs received three U.S. Department of Commerce Gold Medals for Distinguished Achievement.

Alain Rüfenacht was born in La Chaux-de-Fonds, Switzerland, in 1975. He received the Ph.D. degree from the University of Neuchâtel, Switzerland, in 2005, for his work, in collaboration with the IBM Zurich Research Laboratory, on high-temperature superconducting ultrathin films.

In 1999, he was a Scientific Collaborator with the Electrical Quantum Standards Laboratory, Federal Office of Metrology (METAS), Bern-Wabern, Switzerland. In 2007 and 2008, he was a Guest Researcher with the Quantum Voltage Project, National Institute of Standards and Technology, Boulder, CO, USA, focusing mainly on the integration of Josephson junction arrays into voltage standards. Since 2009, he has been with METAS, working on the capacitance standard charged with single electron pumps and on Josephson voltage standards.

Samuel P. Benz (M'01–SM'01–F'10) was born in Dubuque, IA, USA, on December 4, 1962. He received the B.A. degree (*summa cum laude*) in physics and mathematics from Luther College, Decorah, IA, USA, in 1985, and the M.A. and Ph.D. degrees in physics from Harvard University, Cambridge, MA, USA, in 1987 and 1990, respectively.

In 1990, he joined the National Institute of Standards and Technology (NIST), Boulder, CO, USA, as an NIST/NRC Post-Doctoral Fellow and became a permanent Staff Member in January 1992. He has been the Project Leader of the Quantum Voltage Project at NIST since October 1999. He has worked on a broad range of topics within the field of superconducting electronics, including Josephson junction array oscillators, single flux quantum logic, ac and dc Josephson voltage standards, Josephson waveform synthesis, and noise thermometry. He has authored over 160 publications and is the holds three patents in the field of superconducting electronics.

Dr. Benz is a Fellow of the APS, and a member of Phi Beta Kappa and Sigma Pi Sigma. He has received three U.S. Department of Commerce Gold Medals for Distinguished Achievement and the 2006 IEEE Council on Superconductivity Van Duzer Prize. He was awarded an R. J. McElroy Fellowship between 1985 and 1988 to work toward the Ph.D. degree.

Paul D. Dresselhaus was born in Arlington, MA, USA, on January 5, 1963. He received the B.S. degree in physics and electrical engineering from the Massachusetts Institute of Technology, Cambridge, MA, USA, in 1985, and the Ph.D. degree in applied physics from Yale University, New Haven, CT, USA, in 1991.

In 1999, he joined the Quantum Voltage Project at the National Institute of Standards and Technology, Boulder, CO, USA, where he has developed novel superconducting circuits and broadband bias electronics for precision voltage waveform synthesis and programmable voltage standard systems. He was with Northrop Grumman for three years, where he designed and tested numerous gigahertz-speed superconductive circuits, including code generators and analog-to-digital converters. He also upgraded the simulation and layout capabilities at Northrop Grumman to be among the world's best. He has also been a Post-Doctoral Assistant with State University of New York, Stony Brook, NY, USA, where he worked on the nanolithographic fabrication and study of Nb–AlOx–Nb junctions for single-electron and SFQ applications, single-electron transistors and arrays in Al–AlOx tunnel junctions, and the properties of ultrasmall Josephson junctions.

Dr. Dresselhaus received two U.S. Department of Commerce Gold Medals for Distinguished Achievement and the 2006 IEEE Council on Superconductivity Van Duzer Prize.